

# Correcting TLEs at Epoch: Application to the GPS Constellation \*

Delphine Ly<sup>a</sup>, Romain Lucken<sup>a,b,\*</sup>, Damien Giolito<sup>a</sup>

<sup>a</sup>Share My Space, 1 mail Gay-Lussac 95000 Neuville-sur-Oise, FRANCE

<sup>b</sup>Laboratoire de Physique des Plasmas (LPP), UMR CNRS 764, Ecole Polytechnique, Route de Saclay 91128 Palaiseau, FRANCE

---

## Abstract

Two-Line Elements (TLEs) issued by the space-track catalog are still the most extensive public data source for space debris tracking to date. However, TLEs accuracy at epoch is typically larger than 1 km in Low Earth Orbit (LEO) and 3 km in Medium Earth Orbit (MEO). Therefore, TLEs are too coarse to enable collision avoidance maneuvers. The present work aims at correcting TLEs orbits at epoch to enable operational conjunction assessment and help satellite operators better protect their assets at moderate cost.

Using only Moon-Earth and Sun-Earth distance time series, as well as 2018 TLE data for 14 GPS satellites and SGP4 propagation over a short period, we were able to correct the TLEs of the 29 operational GPS satellites by 65% on average for year 2019, reducing the 3D RMS error at epoch from 2.2 km to 680 m. In other words, we improved TLEs accuracy from 5km to 1.5km with a 95% confidence level.

*Keywords:* TLE error, GPS satellites trajectories, Mean orbital elements

---

## Introduction

Since the Iridium 33/Cosmos 2251 collision of January 2009, the JSpOC (US Air Force) has been sending conjunction data messages (CDMs) to satellite operators when a collision probability greater than typically  $10^{-4}$  is identified. The JSpOC maintains the most extensive Earth-orbit objects catalog ("Space-Track"), tracking about 23,000 objects larger than 10 cm, based on optical and RADAR observations made by a network of 25 sites worldwide. Among these objects, 18,000 are in LEO and 5% only are active satellites. However, the Space-Track catalog does not provide accuracy and covariance information along with TLEs.

Precise orbits data is publicly available for some satellites, allowing for TLE error assessment. As an example, TLE 3D root mean square (RMS) error on Sentinel-1A, orbiting in LEO, is approximately 1 km, while the error on the MEO GPS satellites averages 3 km. This initial error (sometimes called "bias") must be distinguished from the propagation error – although they are not exclusive. TLEs provide Brouwer-Lyddane mean elements, which can be converted to Keplerian elements by reconstituting the removed oscillating parts with the SGP4 propagator. Moreover, latest observations are not published as such, but averaged with positions propagated from past TLEs using the SGP4 propagator, and published only if the difference with the propagated positions exceeds 5 km for NORAD objects [1]. Therefore the error at epoch stems at once from the SGP4 physical approximations (such as minimizing the effect of the atmospheric drag), observation network deficiencies and data processing methods.

The SGP4 is a general perturbations analytical propagation model developed in the sixties to trade accuracy for computation speed, specifically designed to handle TLEs (and vice versa). The use of the SGP4 in the generation of new TLEs adds on a modeling error to the observation error. Moreover, it is not clear whether the timescale used for the observations is UTC or UT1 [1], and it might depend on the observation site. Hence, TLE ephemerides at epoch are usually referred to as *pseudo-observations*.

---

\*This paper was presented during the First International International Orbital Debris Conference in Sugar Land, Texas

\*Corresponding author

*Email addresses:* delphine.ly@sharemyspace.global (Delphine Ly), romain.lucken@sharemyspace.global (Romain Lucken), damien.giolito@sharemyspace.global (Damien Giolito)

Because of TLEs low accuracy, LEO satellites operators receive up to one hundred CDMs per day and per satellite from the JSpOC, the vast majority of them false alerts. In these circumstances, a true positive can possibly go unnoticed.

There is ongoing research on modeling the prediction error of physics-based propagators using machine learning (San Juan et al., 2017 [2] or Peng and Bai in 2018 [3]). For now, it does not improve TLEs accuracy less than 2-3 days after the epoch to our knowledge, due to coarse initial conditions. As collision avoidance manoeuvres are usually done 1 to 3 day before the event's predicted occurrence, an operationally viable collision avoidance system must be sufficiently accurate in the short term.

In this paper, we focus on improving TLEs accuracy at epoch, in line with the work done by Levit and Marshall in 2011 [4] or Sang et al. in 2013 [5]. The corrected pseudo-observations can then be propagated with machine learning-enhanced techniques, to yield better prediction in the future. Our approach consists in identifying and exploiting correlations between a history of orbital and physical parameters and the TLEs error, using statistical and machine learning techniques. As satellites in MEO have a more stable and easily predictable trajectory, we chose the GPS constellations to first develop and test this data-driven approach. The ultimate goal being to generalize to LEO satellites, then to space debris.

We first present the data sets and preprocessing steps in Section 1. In Section 2, we summarize the preliminary analysis we conducted on the GPS TLEs error. In Section 3, we describe our method to correct the along-track position of a given TLE orbit and present our model's performances on 2019 GPS data.

## 1. Data description and preprocessing

### 1.1. The GPS constellation

The GPS constellation was deployed in 1973 for military purposes, became fully operational in 1995 and opened for civil use in 2000. As of today, 29 GPS satellites are fully operational.

#### 1.1.1. GPS characteristics

GPS satellites fly at an altitude of 20 180 km in a near-circular orbit at a speed of about 4 km/s, with a 718 minutes revolution period. They share the same nominal inclination of  $55^\circ$  but are distributed among 6 orbital planes, equally spaced by  $60^\circ$  RAAN.

Altitude	20 180	km
Inclination	55	$^\circ$
Eccentricity	$\sim 1$	%
Period	718	min

Table 1: GPS constellation nominal orbit properties.

Currently operational satellites were launched between 1997 and 2016. Among them, 19 are block IIR or IIR-M types: they have a launch mass of 2 030 kg, for a size of  $1.7 \times 11.4$  m. The 10 others are block IIF type, with a launch mass of 1 630 kg and a size of  $2.4 \times 35.5$  m. All of them are three-axis stabilized.

#### 1.1.2. IGS precise orbit (the "truth" data)

The international GNSS Service collects and distributes GPS observation data, which can be accessed through the CDDIS FTP server (<ftp://cddis.gsfc.nasa.gov/gnss/products/>). The highest quality IGS products are the Final orbits files, with a 3.5 cm 3D RMS accuracy. We consider it the "truth" data. They are made available with a delay of up to 20 days, in the Standard Product 3 (SP3) format. Those precise orbits files provide position vectors at a 15 min rate, referenced to the ITRF frame and GPS time. Velocities are not provided.

### 1.1.3. GPS TLEs publication

New TLEs for GPS satellites are published at a rate ranging from 780 minutes to 1 200 minutes on average, corresponding to 1.1- 1.7 revolutions. There seems to be a correlation between the TLEs publication rate and the orbital plane, but we did not investigate this further.

It appears that for some GPS satellites, TLEs are published only when they cross the equatorial plane in the North Pole direction.

## 1.2. Data preprocessing

For the scope of this work, we extracted the constellation's IGS and Space-Track orbits from January 2018 to the beginning of October 2019.

### 1.2.1. Removing outliers

The only outliers that were filtered out were TLE data with a 3D error exceeding 10 km, which was possibly caused by a manoeuvre. At most two data points per satellite were removed this way, but for the vast majority of the satellites, there were no outliers in the given period of time.

### 1.2.2. Interpolating and differentiating

To evaluate the TLEs error, we interpolated IGS Final orbits at TLEs epochs, following the guidelines recommended in Horemuz et al., 2006 [6]. Namely, interpolating to the 16<sup>th</sup> degree Lagrange polynomial, with the target epoch falling in the middle of the interpolation range to avoid Runge's Phenomenon effect. The method was tested by interpolating on existing data that were purposely skipped at fitting time. The error was found to be at the centimeter-level.

The velocity vectors  $\mathbf{v}$  were computed by central differentiation of the position vectors  $\mathbf{x}$ :

$$\mathbf{v}(t) = \frac{\mathbf{x}(t + \epsilon) - \mathbf{x}(t - \epsilon)}{2\epsilon} \quad (1)$$

with  $\epsilon = 10^{-8}$  s.

The Astropy library was used to compute Moon and Sun ephemerides (DE432 kernels) and for Cartesian reference frame transformations (ITRF08 and J2000 GCRF).

## 2. Preliminary analysis of GPS TLEs error

### 2.1. Selecting orbital parameters to be corrected

Rather than considering the error as a whole, our strategy was to divide it into several components, and focus on the component accounting for the largest part of the error. As noticed by several authors (e.g. [2] and [7]), when splitting the TLEs error between its along-track, radial and cross-track components, the along-track component (here denominated  $\phi$ ) shows the highest uncertainties. To estimate the exact proportion to which the error could be reduced by correcting solely  $\phi$  compared to other orbital parameters, we calculated the error after correction of each of them separately (here denominated the "residual error").

As shown in Table 2, the along-track error is responsible for nearly 90% of the total error on average for the whole constellation in 2018, making it a key parameter to improve. On the contrary, due to the hierarchy between Keplerian parameters, correcting only the semi-major axis can lead to an increase of the 3D error. Correcting the inclination and the RAAN has little to no effect on the error reduction.

Corrected parameter	None	Semi-major axis	Inclination	RAAN	$\phi$
Residual error [km]	2.06	2.08	2.06	2.01	<b>0.25</b>
% Improvement	0	-1	0	2	<b>88</b>

Table 2: Residual error after correction of a single orbital parameter in 2018.

2.2. Decomposing the along-track error trends

The error on the along-track position is plotted in Figure 1 (top) together with the temporal evolution of the Moon-Earth distance (bottom). Several features are observed:

- The error has a periodical component that corresponds approximately to the moon cycle. The amplitude and the phase of these fluctuations remain almost constant in time and from one satellite to another.
- The time-averaged error is of the same order as the amplitude of the fluctuations. The mean error strongly varies from one satellite to another. It can be either positive or negative.

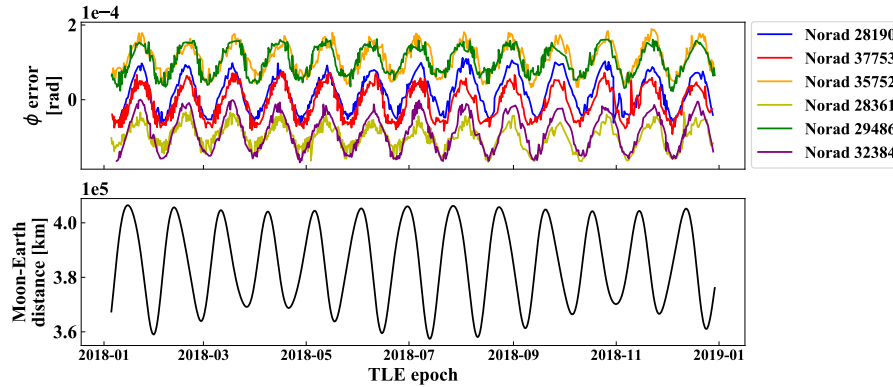


Figure 1: Along-track error for 6 GPS satellites on different orbital planes and Moon-Earth distance. Both II-R/M and IIF blocks are represented.

A Seasonal and Trend decomposition is applied to the along-track error using Loess [8] algorithm. We obtained similar seasonal patterns for every GPS, and mean values ranging from  $-1.5 \times 10^{-4}$  to  $1.5 \times 10^{-4}$  radians. In the following,  $\phi$  SE error stands for the seasonal error of the along-track position, and  $\phi$  ME error stands for the mean error of the along-track position.

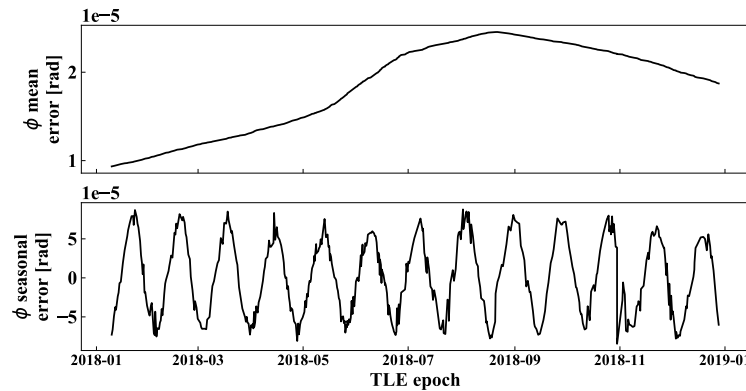


Figure 2: USA-177 (NORAD 28190) along-track mean and seasonal error trends.

3. Correcting TLEs along-track error

3.1. Methodology

In order to test the generalization capabilities of our model, we selected 14 GPS (referred to as the "training set") spread over five different orbital planes and two different block types (see full description in Appendix A), to use for assumptions making, statistical analysis and fitting. We then evaluated the accuracy of the resulting model on the remaining 15 satellites, first in 2018, then in 2019.

3.2. Correcting the seasonal variations

Correlation to the Moon cycle

Noticing that the seasonal trend seemed correlated to the lunar cycle (as shown in Figure 1), we first modeled the seasonal error of the whole training set by Nadaraya-Watson kernel regression [9], with a kernel bandwidth of 0.1. We used JPL DE432 ephemerides to obtain a Moon-Earth distance interpolation function for years 2018 and 2019. We then calculated the shift between the resulting signal and the Moon-Earth distance signal, taking August 5, 2018 as an arbitrary reference date from which to compare both signals. We shifted the Moon-Earth distance signal by the resulting value (the "Moon -  $\phi$  SE shift"), so that the signals were in phase.

As shown in Figure 3, we found a quadratic (nearly linear) relation between the Moon-Earth distance and  $\phi$  shifted seasonal error values.

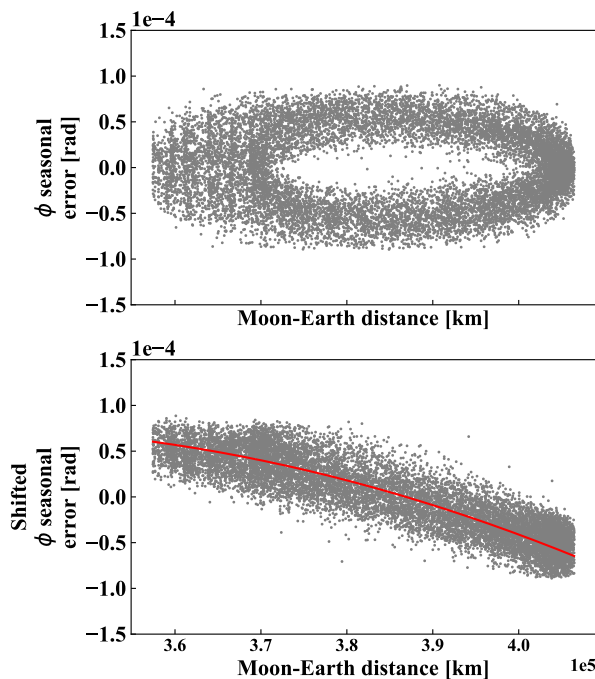


Figure 3: Along-track seasonal error as a function of Moon-Earth distance in 2018.

We will refer to the resulting regression polynomial as the "Moon -  $\phi$  shifted SE" polynomial further on.

Correlation to the Sun cycle

When running predictions using the aforementioned shift value and regression coefficients on the training set, it appeared that part of the prediction error obviously stemmed from a bad shift calibration at some periods of the year, while it was working well at others, according to a roughly biannual pattern. Rather than using a constant shift value throughout the year, we explored external phenomena that could help us refine our shift estimation at any time of the year. We took 12 reference dates in 2018, equally spaced by the mean anomalistic month period (i.e. 27.55455 days), and calculated the shift value at each period. We found a quadratic relation between the solar cycle and the 12 resulting shift values (Figure 4).

We will refer to the resulting regression polynomial as the "Sun-Earth distance - Shift" polynomial.

To compute the regression between  $\phi$  shifted seasonal error and the Moon-Earth distance, we cross-validated different shift values on the training set and selected the one leading to the best regression performance (measured by  $r^2$  score). It was found to be the mean value of the 12 shift values computed at each anomalistic month. We updated the Moon -  $\phi$  shifted SE polynomial with the coefficients of the regression performed after shifting the Moon-Earth distance signal by the optimized shift value.

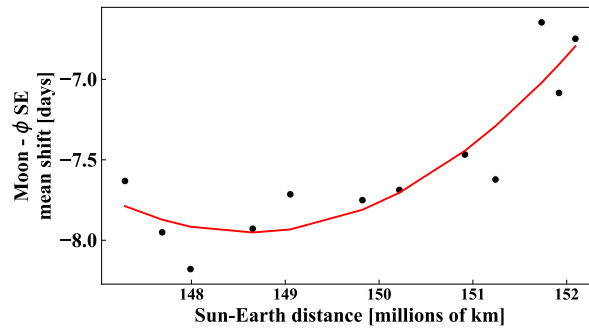


Figure 4: Moon -  $\phi$  SE mean shift as a function of Sun-Earth distance by anomalistic month in 2018.

### 3.3. Correcting the mean error

We were able to identify a functional form linking the along-track mean error to an orbital characteristic that we denominated  $\mathcal{F}$ , which can be obtained by propagating the orbit over the next few hours after epoch using SGP4.

### 3.4. Running predictions

At prediction time, only two types of values must be provided to the model: the orbital parameters used in the  $\mathcal{F}$  functional form, and the Sun-Earth distance (in millions of km) at the targeted epoch. The error prediction is performed by the following sequence:

1. The along-track mean error is computed by applying the  $\mathcal{F}$  functional form to the orbital data.
2. The shift value is computed by applying the Sun-Earth distance - Shift regression polynomial coefficients to the Sun-Earth distance at epoch.
3. The Moon-Earth distance value is shifted by applying a Moon-Earth distance interpolation function to  $t=epoch+shift$ .
4. The along-track seasonal error is obtained by applying the Moon -  $\phi$  shifted SE regression polynomial coefficients to the shifted Moon-Earth distance.
5.  $\phi$  mean and seasonal error predictions are finally summed up to predict the along-track error.
6. The residual 3D error is evaluated after correction of the along-track component with the predicted error.

### 3.5. Results

We ran predictions on year 2019 (up to October 1<sup>st</sup>) TLEs of the 15 GPS satellites excluded from the analysis, and corrected their position accordingly. The corrected orbits improved TLEs accuracy at epoch by 63% on average.

NORAD	TLE error [km]	Prediction error [km]	% Improvement
40730	2.39	0.88	63.37
39166	1.69	0.86	48.99
39741	2.77	0.54	80.39
35752	2.78	0.51	81.55
28129	4.09	1.28	68.58
40294	3.12	0.7	77.46
26360	1.14	0.54	52.93
41019	1.08	0.66	39.11
41328	1.53	0.69	54.62
32260	2.5	0.72	71.27
24876	0.99	0.55	44.25
40105	2.96	0.54	81.73
32711	1.17	0.88	24.78
39533	1.98	0.7	64.71
29601	2.53	0.72	71.35
40534	2.46	0.66	73.4
27663	2.37	0.54	77.21

Table 3: Year 2019 predictions for the satellites that are not in the training set.

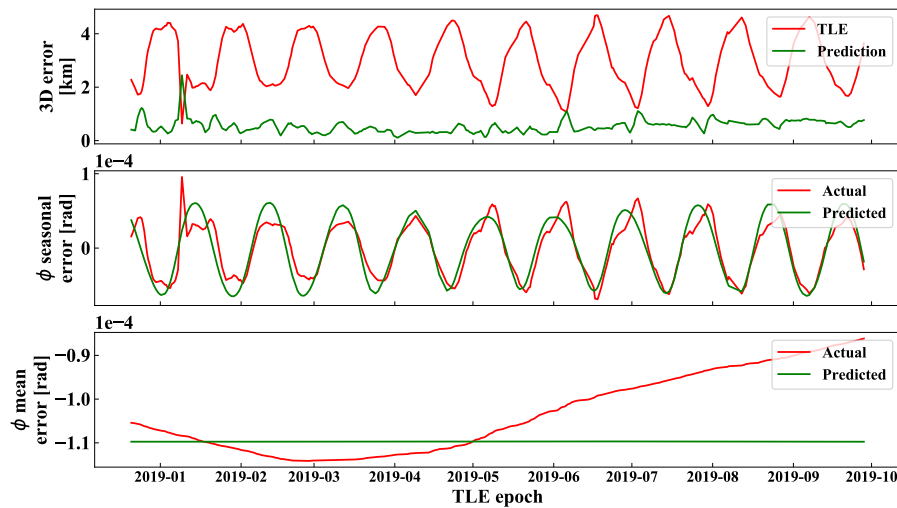


Figure 5: Broken down predictions for USA-256 (NORAD 40105).

### Conclusion

By performing a statistical analysis on a subset of 14 GPS satellites over the year 2018, we were able to improve the TLEs of the 15 satellites of the test set by 63% for year 2019. Further improvements could involve higher harmonics of the Moon and Sun motions, or the correction of other orbital parameters by similar methods.

TLEs error at epoch depends on the orbit type. The obtained fitting coefficients are not expected to match well the error made on highly eccentric orbits or LEO for instance. However, it appeared that most of the error made on the TLE can be corrected with only a limited number of parameters and simple statistical tools. The method developed in this paper will be applied to LEO satellites and LEO debris, possibly using machine learning techniques. After sample validation through direct observation, corrected TLEs orbits are intended to be used for conjunction assessment in the future.

## Acknowledgments

This work has received financial support from the French public investment bank BPI France and the Île-de-France region through the Innov'up 2019 program.

## References

- [1] D. Vallado, P. Crawford, R. Hujsak, and T.S. Kelso. Revisiting Spacetrack Report # 3: Rev. *AIAA/AAS Astrodynamics Specialist Conference and Exhibit*, (6753), 2006.
- [2] J. F. San-Juan, I. Pérez, M. San-Martín, and E. P. Vergara. Hybrid SGP4 orbit propagator. *Acta Astronautica*, 137:254–260, 2017.
- [3] H. Peng and X. Bai. Improving Orbit Prediction Accuracy through Supervised Machine Learning. *Advances in Space Research*, 61(10):2628–2646, 2018.
- [4] C. Levit and W. Marshall. Improved orbit predictions using two-line elements. *Advances in Space Research*, 47(7):1107–1115, 2011.
- [5] J. Sang, J. C. Bennett, and C. H. Smith. Estimation of ballistic coefficients of low altitude debris objects from historical two line elements. *Advances in Space Research*, 52(1):117 – 124, 2013.
- [6] M. Horemuž and J. Andersson. Polynomial interpolation of gps satellite coordinates. *GPS Solutions*, 10:67–72, 02 2006.
- [7] D. Racelis and M. Joerger. Correction: High-integrity tle error models for meo and geo satellites. *2018 AIAA Space and Astronautics Forum and Exposition*, (5241), 2018.
- [8] R. B. Cleveland, W. S. Cleveland, J. E. McRae, and I. Terpenning. STL: A seasonal-trend decomposition procedure based on loess (with discussion). *Journal of Official Statistics*, 6:3–73, 1990.
- [9] E. A. Nadaraya. On estimating regression. *Theory of Probability & Its Applications*, 9(1):141–142, 1964.

## Appendix A.

Norad	Launch year	Orbital plane	Block type
28190	2004	5	IIR
28874	2005	4	IIR-M
32384	2007	1	IIR-M
37753	2011	2	IIF
27704	2003	3	IIR
25933	1999	5	IIR
28474	2004	1	IIR
28361	2004	4	IIR
26605	2000	5	IIR
29486	2006	2	IIR-M
36585	2010	2	IIF
27663	2003	1	IIR
35752	2009	3	IIR-M
26407	2000	3	IIR

Table A.4: Characteristics of satellites used for training.